Chapter 1
Quantities and Fundamental Units of External Dosimetry

Abstract In this chapter, the radiation field is characterized in terms of energy and flux at a point of space. These physical datas than make possible to obtain the radiometric and dosimetric quantities of reference for external exposure, such as: fluence, kerma for the indirectly ionizing radiations and the dose. In addition, other quantities such as linear energy transfer and relative biological effectiveness are detailed; they relate to the effect of radiation on biological tissues and to the damage that can occur at the cellular level.

Initially, we will attempt to define the characteristic quantities of dosimetry and radiation fields, called radiometric quantities. The fundamental radiometric and dosimetric quantities are essentially threefold:

- Fluence Φ;
- Absorbed dose D;
- Kerma K.

We will note that these quantities were defined by the ICRU (International Commission on Radiation Units and measurements) as transition variables in obtaining protection and operational quantities (detailed in Chaps. 2 and 3), they are measurable and above all they correspond to punctual concepts. Add to that two other intermediate variables that will be particularly suitable in the dose-biological effects relationship: The linear energy transfer (LET) and the relative biological effectiveness (RBE). All these quantities are detailed in the following.

1.1 Dosimetric Quantities

1.1.1 Total Absorbed Dose and Linear Energy Transfer

Biological dosimetry will consist initially to characterize the physical dose deposited in human tissue. This approach is immediately responsible for a dual problem that

R. Antoni and L. Bourgois, *Applied Physics of External Radiation Exposure*,
Biological and Medical Physics, Biomedical Engineering,
DOI 10.1007/978-3-319-48660-4_1

we will discuss: "typology" of energy deposition as a function of radiation type and size of the volume of tissue in which is characterized this deposition.

In the first approach, for a macroscopic context, i.e. a volume V surrounding a mass m of material sufficiently large (tissue level), subject to radiation responsible for a deposited energy E, the dose is defined by the expression (1.1).

$$\overline{\mathrm{D}} = \frac{\mathrm{E}}{\mathrm{m}} \tag{1.1}$$

In the international system, this quantity is consistent with J kg^{-1} but his unit, the gray (Gy), comes from the name of one of the founding fathers of dosimetry (1 Gy = 1 J kg^{-1}). The bar on the variable D indicates that the result of this calculation is an average: no matter the "topology" of deposited dose. In other words, no matter how the mass m has been irradiated, in homogeneous way or not, the final result is averaged over the total mass. This macroscopic quantity will be called later in the book: "total deposited dose." Without details, we will say that energy depositions are the result of excitations, ionization and generally the setting in motion of any secondary charged particle (e.g. electrons for photons, recoil nuclei for neutrons). The total number of ionizations and excitations can be extremely important and can reach the order of 10^5 for a dose of 1 Gy in a volume the size of the cell nucleus.

Once the dose determined, the "typology" of the deposited dose along the path of the incident particle is then decisive because it greatly influences the response of the medium crossed in this case of human tissues. Indeed, one of the major limitations of the approach leading to such a dose as defined in (1.1) is the failure to take into account the geometry of the energy deposition in the target volume. In particular, it is clear that understanding of the action of radiation on the biological material requires information on the scale of the DNA, that is to say to lower target dimensions less than micron.

It has been found indeed that for equal amount of energy absorbed, the effect depends on the nature of the incident particle. For a certain type of radiation such as photons, electrons and protons to high energies, the location of ionization and excitations are separated in space. However, for low-energy protons, neutrons and ions, ionization are relatively clustered in close proximity of the passage of the particle into tissue. Figure 1.1 shows a schematic view of the difference in density of ionization and excitation to the same sensitive volume and for photons and ions.

The physical quantity to characterise the ionization density disparity depending on the type of radiation and therefore the effects on biological tissues, is the ratio of the deposited energy per unit of path length in the material. For a macroscopic approach, this means, in a given environment, to determine the amount of energy ΔE lost by the particle on a portion of its path Δl.

$$\overline{L} = \left(\frac{\Delta E}{\Delta l}\right) \tag{1.2}$$

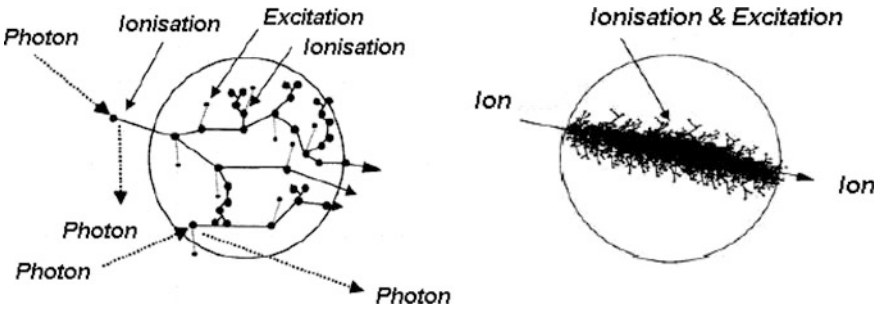

Fig. 1.1 Schematic representation of a photon track and ion through a cell, showing the difference in density of energy deposition in both cases [1], with permission from Springer Heidelberg

In the international system, this quantity is consistent with J m^{-1}, but found in several nuclear units (keV μm^{-1} keV cm^{-1} …). By making infinitesimal terms of the ratio of (1.2) we get the quantity called "linear energy transfer".

$$\lim_{\Delta l \to 0} \overline{L} = L = \left(\frac{dE}{dl} \right) \tag{1.3}$$

This quantity has the same unit as the last. In the literature, we can also find it expressed as a "infinite LET" with the following symbol: L_∞ meaning that the total loss of energy is taken into account through the passage of the particle in matter and not just a fraction confined to the periphery near the passage; by default, L equals L_∞. The LET is a non-stochastic quantity that does not account for the discontinuous nature of energy transfers and statistical fluctuations, as the total deposited dose. It expresses the mean energy loss for a large number of particles. We will see later the incidence of this quantity on cell survival.

Let us add that this quantity is similar to the physical quantity of the "Stopping Power" S for the charged particles and that there are analytical expressions depending on the energy of the incident particle and the type of particle to characterize it that will be detailed in the remainder of this book. By definition, the dose is essentially a deposited energy density. In our initial macroscopic approach leading to the expression (1.1), we can easily make an analogy with the mass density of a material. Recall that the mass density at a point is mathematically considered as the ratio of the mass contained in a element of volume surrounding that point. If the matter was continuous and homogeneous, this ratio does not depend on the size of the element of volume. Against by the fact that a material is composed of discrete entities (atoms, molecules) implies that the volume should contain a sufficiently large number of these entities so that density is a reliable statistical significance. For example, to a volume corresponding to an atom, the concept of density becomes ill-defined and the estimated density at this scale can be very variable.

Microdosimetry focuses precisely quantify the distribution of energy deposition at the microscopic level for sensitive volumes of the order of the cell (10 μm). This discipline has grown significantly to include, among others, how are induced biological effects at the cellular level and in particular to explain the dose-response curves.

The statistical fluctuation of energy deposits was clearly illustrated by Rossi [2] considering, as shown in Fig. 1.2, a set of 150 cells (5 μm diameter) exposed to various types of radiation fields: on the left 1 MeV photons and on the right 1 MeV fission neutrons. The secondary particles from the neutron (mainly the protons of hydrogen from tissues) have a limited path of a few diameters of the cell.

The secondary electrons from the gammas have a greater path than the overall area containing all the cells. The path length traversed in total by the electron is 200 times greater than that of the protons moved by neutrons. Accordingly, the energy deposition actually impacts only very few cells in the case of the interaction of 1 MeV neutrons.

Since the response of a cell depends on the energy absorbed per unit mass, it is essential to consider the fluctuations of the energy per affected cell. An absorbed dose of 10 mGy implies a mean energy per cell equal to the product of 10 mGy by the mass of a cell, but there is a difference in the distribution of energy deposition by cell.

In the case of photon irradiation, fluctuating energy per cell is low and we can consider that we are essentially in a continuous medium. The total deposited dose, as defined by the expression (1.1) as average, takes sense in. for neutrons, fluctuations are significant; 98% of the cells do not get energy and some get significant energy (about 50 times the average). The expression of the total deposited provide this tissue an extremely partial information about the "topology" of déposited dose. In what follows, we will define the microdosimetric concepts enable to understand the dose deposition across the cell.

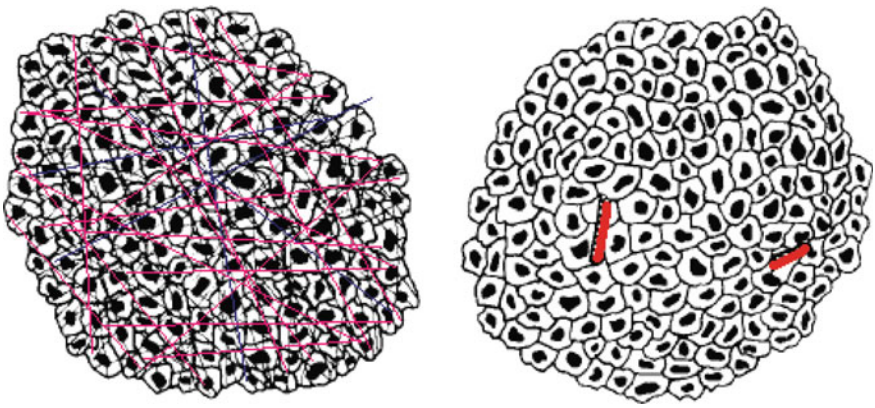

Fig. 1.2 Representation of a 10mGy dose delivered from gamma ^{60}Co (*left*) and the same dose delivered by 1 MeV neutrons (*right*) in a cell volume of 150 cell of 5 μm diameter [2], with permission from Springer Heidelberg

1.1.2 Fundamental Quantities of Microdosimetry and Definition of the Absorbed Dose

Most physical microdosimetry quantities were defined and standardized by the International Commission on Radiation Units and Measurement in the report of the ICRU report 36 [3]. First, the term "event", written the meaning of microdosimetry, represents the whole of energy deposition in the sensitive volume considered, produced by the incident particle and all its secondary particles being moved. "The energy imparted" is defined by the expression (1.4).

$$\varepsilon = \sum \mathrm{E_e} - \sum \mathrm{E_s} + \sum \mathrm{Q_{\Delta m}} \tag{1.4}$$

In other words, for a given volume V, ε is given by the whole of energies of all incoming particles (E_e), which is subtracted from all the energies of all outgoing particles (E_s). The heat reaction term $Q_{\Delta m}$ reflects the change in mass of all particles and nuclei involved in nuclear interactions in the sensitive volume. In human tissue, this term is substantially negligible. Note that ε is a stochastic quantity subject to statistical fluctuations of the interactions of incident particles with secondary particles being moved. To reach a mean value of the energy imparted, it should be to perform a large number of measures or to consider a large enough volume to make these significant statistical fluctuations. From this quantity, a stochastic variable is defined similar to the dose defined by the expression (1.1), but this time for a microscopic approach adapted to dimensions of the order of the cell. This is the "specific energy". It is calculated by the ratio of the energy imparted and the mass of the sensitive volume according to expression (1.5).

$$z = \frac{\varepsilon}{m} \tag{1.5}$$

It is also expressed in gray (Gy); m is the mass of the sensitive site; from the point of microscopic view we prefer to speak of "sensitive site" rather than sensitive volume because of the small dimensions likely to be affected (e.g. cell nucleus). This quantity characterizes the local energy deposition.

The total deposited dose $\overline{D}$ is a non-stochastic quantity: when the measurement is repeated, the values obtained are in each case identical with deviation due to measurement accuracy. However, fluctuations in z are important and originate from the fact that energy deposition are due to discrete events, the number decreases as the size of the sensitive site decrease.

Figure 1.3 shows the field of the microdosimetry, which is located in the part where the fluctuations in energy deposition are significant. This section relates to sensitive sites of low mass, so small size.

To go from the specific energy to the total deposited dose D expression (1.1) a "distribution of the specific energy dependent D" is defined.

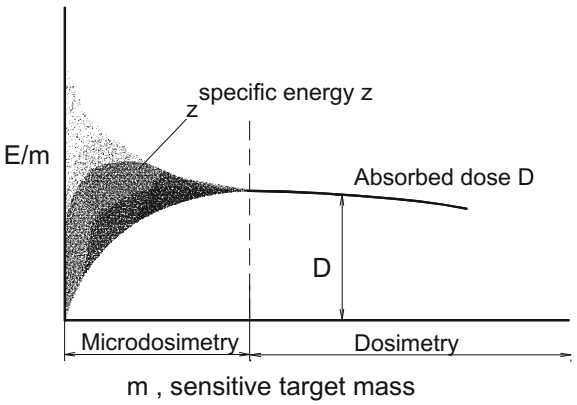

Fig. 1.3 Representation of the variation of the specific energy z depending on the mass m sensitive site

When a small sensitive volume (in the range of one nanometer or micrometer) receives the energy deposition of several events (single or multiple) different values of the specific energy are recorded. For a large number of consecutive events, fluctuations of the specific energy can be represented by a probability density function, $f\left(z,\overline{D}\right)$, where $\overline{D}$ represents the total dose deposited to a small volume. The cumulative probability density associated $F\left(z,\overline{D}\right)$ is the probability that the specific energy is less than or equal to z.

$$\mathrm{F}\left(\mathrm{z},\,\overline{\mathrm{D}}\right)=\mathrm{P}\quad\left(0\leq\mathrm{z}'\leq\mathrm{z},\,\overline{\mathrm{D}}\right) \tag{1.6}$$

$$\mathrm{f}\left(\mathrm{z},\,\overline{\mathrm{D}}\right)=\frac{\mathrm{dF}\left(\mathrm{z},\,\overline{\mathrm{D}}\right)}{\mathrm{dz}} \tag{1.7}$$

The total deposited dose, corresponding *de facto* to a specific mean energy, is then obtained by average of the distribution as (1.8).

$$\overline{D}=\overline{z}=\int z\cdot f\left(z,\overline{D}\right)dz \tag{1.8}$$

By performing this average, we pass from a stochastic quantity subject to statistical fluctuations to a mean macroscopic quantity consistent with the expression (1.1).

$$\overline{\mathrm{D}}=\frac{\bar{\varepsilon}}{\mathrm{m}} \tag{1.9}$$

Finally, if we reach the mass of this object to a negligible amount, we get the "absorbed dose", this time corresponding to a punctual characterization of the dose.

$$\lim_{\mathrm{m}\to 0}\overline{\mathrm{D}}=\frac{\mathrm{d}\bar{\varepsilon}}{\mathrm{dm}}=\mathrm{D} \tag{1.10}$$

This quantity is a fundamental dosimetric variable. while punctual in nature, we will show later that it is measurable and calculable. It is obvious that in an irradiated macroscopic inhomogeneous medium the value of the absorbed dose varies from one point to another in the volume. The latter therefore overcomes, in part, the "topology" of the deposited dose. From this quantity, we define a "absorbed dose rate" (1.11) homogeneous to Gy s^{-1}.

$$\dot{D} = \frac{dD}{dt} \tag{1.11}$$

This variable is also a point-quantity. Now, let us get back to the "typology" of energy deposition mentioned above. The LET, while calculated with varying degrees of simplifying assumptions (e.g. linear stopping power for charged particles), has the drawback of not being accessible to the measure. To overcome this limitation, as to the specific energy for the total deposited dose, there is a similar stochastic variable for LET. This variable is calculated using the ratio of the energy imparted to the sensitive site by a single event, to the mean length of the chord in the sensitive site in question according (1.12).

$$y = \frac{\varepsilon}{\bar{l}} \tag{1.12}$$

This quantity is called "lineal energy". As it relates to sensitive sites of the order of microns, it will be expressed in keV μm^{-1}. The microscopic site where happens the energy transfer can be likened to a sphere. The mean chord is then obtained by the ratio of the volume *V* of the sphere to that of the surface at equatorial disk of the sphere (see Chap. 2, Further Details 2.2).

$$\bar{l} = \frac{2}{3}d \tag{1.13}$$

with *d* the diameter of the sensitive site. Unlike the specific energy, we note that this quantity is meaningful only for a single event and not for multiple events. Then, we can readily express the specific energy as a function of that quantity. For material with density of 1 (of the order of that of human tissue), *z* expressed in Gy, *d* in microns and *there* in keV μm^{-1} we obtain equality (1.14).

$$z = \frac{0.204}{d^2}y \tag{1.14}$$

Since the mean lineal energy represents discrete energy deposition, it is more significant than LET to characterize the "topology" of energy deposition of radiation. However, the ICRP publication 60 [4] recommends the use of LET, more accessible quantity, in particular, we will see in Chap. 2, for obtaining a transfer quantity called quality factor *Q*. LET and lineal energy can however be linked considering whether the TLE match the value of the mean lineal frequency energy

$\overline{y}_f$ or at the value of the mean lineal energy dose $\overline{y}_D$ (see Further Details 1.1). We can also talk in the literature of "mean LET". Table 1.1 gives the values of LET and the number of ionizations per μm in water and for various radiations.

Adding that, a class of detectors: "tissue equivalent proportional counters" (TEPC) measure the lineal energy y and specifically his distribution variable (recalling that it is a stochastic variable) for a given radiation flux (see Further Details 1.1) which is also called "microdosimetric spectrum." These chambers recreate an environment and a sensitive volume close to that of a cell. They deliver an electrical pulse proportional to the energy deposited in the detector volume by the heavy secondary charged particles set in motion in the tissue equivalent wall, by the incident radiation. Note that this is not the photon or neutron that deposit dose, but the secondary particles set in motion by the primary radiation. This distinction, we shall see, is the origin of the definition of dosimetric variables specific to these two types of radiation.

This wall in equivalent tissue material is composed by elementary constituents of human: carbon, hydrogen, oxygen and nitrogen. Secondary particles set in movement in this wall are the electrons to photons. For neutrons, according to the energy of the latter: the recoil protons, hydrogen nuclei, the alpha and proton (n, α) and (n, p) and a more marginally heavy nuclei C, O and N. Microdosimetric spectra are characteristic of incident radiation and may have recognizable peaks, indicating the contribution of a particular secondary particle set in motion in the wall. Figure 1.4 shows the general shape of a microdosimetric spectrum obtained in a mixed radiation field (neutron-photon).

- Region A ($y < 15$ keV μm^{-1}): the dose is due to photons (see Fig. 1, Further Details 1.1).
- Region B (1 keV μm^{-1} < y < 100 keV μm^{-1}): This region corresponds to the proton contribution from neutron-material interactions.
- Region C ($y > 100$ keV μm^{-1}): a significant peak appears in this region for neutron energies above 1 MeV. It is the contribution of heavy recoil nuclei (carbon, nitrogen, oxygen), and the (n, α) whose importance increases with the neutron energy (except for boron and lithium).

Table 1.1 Mean LET and number of ionizations per range unit for different radiations, according [15], with the permission of ATSR

Radiance	Particle charge of the ionization	Means TLE (keV μm^{-1})	Number of ionisations by μm
Electrons > 1 MeV photons	Secondary electrons	0.28	8.5
RX 30–180 kV	Secondary electrons	3.2	100
8 kV RX	Secondary electrons	4.7	145
5 MeV alpha	Alpha	120	3700
400 keV neutron	p + e	35.8	1100
12 MeV neutron	p	9.5	290
1 MeV proton	p	54	2000
10 MeV proton	p	8	250

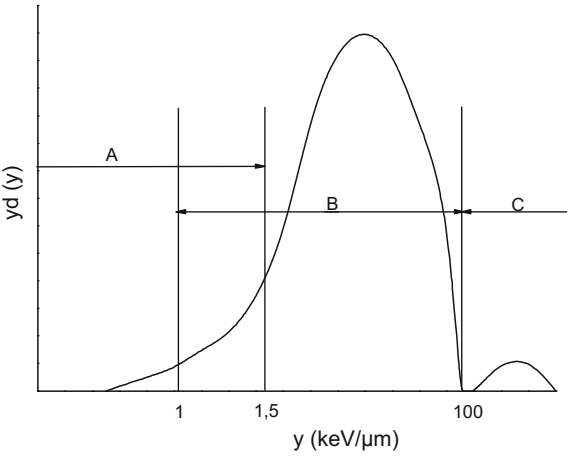

Fig. 1.4 Distribution of typical lineal energy function for a mixed neutron-photon radiation field adapted from [5]

Recovery of spectra for neutrons and photons, between 1 and 15 keV μm^{-1}, encourage to define a threshold at 3.5 keV μm^{-1}. This threshold is effective only in the case of real mixed fields. The check-out of high linear energy beyond 20 keV μm^{-1}, indicates the presence of neutrons. Thus, TEPC allows, to have in real time and with a single measure, a usable information for neutrons and photons; this is one of its main advantages.

Figure 1.5 given a differentiated representation of micro-dosimetric spectra of a TEPC.

For 1 MeV protons, almost only recoil, protons formed by the hydrogen nuclei moved by elastic collision, deposit their energy in the sensitive volume. The maximum energy of the lineal spectrum is around 130 keV μm^{-1}; it is the peak 1, which limits zone 1 and corresponds to the maximum energy deposited by this process when the range of the recoil proton is substantially equal to the diameter of the sensitive volume of the detector (here 2 μm). We note that this peak is common to all three spectra of incident energy. This type of interaction taking place at three energies but with different probabilities of occurrence (cross section inversely proportional to the square root of the energy in this energy range).

Zone 2 is due to inelastic capture (n, α) most likely being the following: $^{14}N(n, \alpha)$ $^{16}O(n, \alpha)$ and $^{12}C(n, \alpha)$ with the following respective response thresholds: 0.16; 2.35 and 6.18 MeV. This explains for 1 MeV neutrons a small contribution in the area 2, a more important for those of 5 MeV, since both reactions are possible. Finally a greater at 15 MeV, because this time the three capture reactions are possible. The optimum of lineal energy, marked by the peak 2, around 300 keV μm^{-1}.

Zone 3 is due to the energy deposition in the sensitive volume of heavy nuclei set in motion in the wall, that is to say: oxygen, carbon and nitrogen. Note that their very small path in the wall limits the number of those entering the gas-sensitive volume, this explains the low amplitude of the area. The maximum peak 3 is around 1000 keV μm^{-1} for neutrons 5 MeV and 1500 keV μm^{-1} for 15 MeV neutrons and indicated by peak 4.

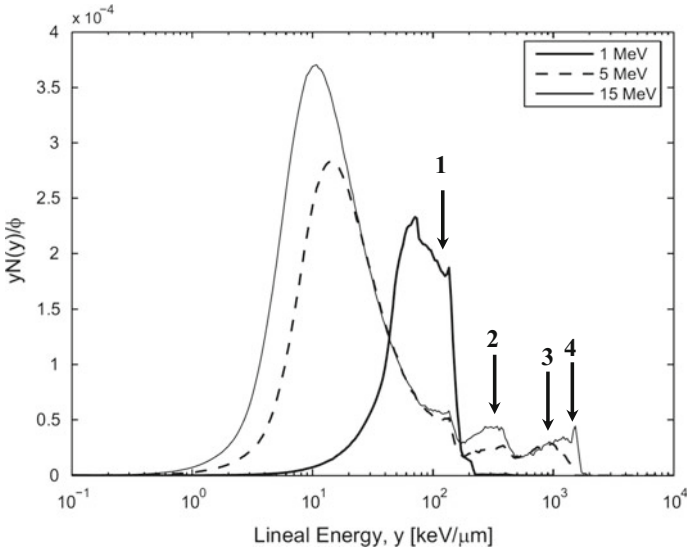

Fig. 1.5 Spectra in a TEPC microdosimetric type detector for different neutron energies: 1, 5 and 15 MeV, reproduced with permission from Elsevier [6]

The spectrum is much larger than in the case of photons. These curves therefore clearly highlight the "mapping" of secondary particles set in movement and the part of energy they deposit in the sensitive volume of the detector supposed to simulate tissue environment cell. At this point, a fundamental distinction in dosimetry related to the type of radiation is involved.

In the case of electrically neutral radiation: photons and neutrons, as briefly mentioned, the secondary particles set in movement are responsible for deposition, electrons in the first and recoil nuclei for the latter. The energy is de facto "indirectly" deposited. This is called "indirectly ionizing radiation." Conversely, the charged particles are called "direct ionizing radiation", since from their penetration into a material medium, they deposit energy "directly" by Coulomb interaction and excitation.

1.1.3 Kerma Calculation for Radiation Indirectly Ionizing

This major difference above is the source of an physical quantity intermediate described as "energy transferred" E_{tr}. It is, this time, not to characterize the deposited energy confined to a sensitive site (ε) but the energy "transferred" to the secondary particles at the point of interaction in the target volume.

To understand the difference between energy imparted ε and energy transferred E_{tr}, consider a photon and an electron microscopic entering a sensitive volume of the dimension of a cell, as shown in Fig. 1.6.

Considering that the path of the electron in the tissue is much greater than the dimensions of the sensitive site, it is possible to assess the mean energy imparted $\overline{\varepsilon}$ on the length of chord through the linear energy transfer TLE. We have recognized that it was possible to define the mean specific energy and thus to the total deposited dose as shown in the expression (1.15).

$$\overline{\mathrm{D}} = \overline{\mathrm{z}} = \frac{\overline{\varepsilon}}{\mathrm{m}} = \frac{1}{\mathrm{m}} \int_{\overline{\mathrm{l}}} \mathrm{L}\,\mathrm{dx} = \frac{1}{\mathrm{m}} \int_{\overline{\mathrm{l}}} \left(\frac{\mathrm{dE}}{\mathrm{dx}}\right) \mathrm{dx} \tag{1.15}$$

Setting the mass to a negligible amount, the absorbed dose D (punctual) is assessable.

Consider by assuming that the incident photon interacts with Compton reaction (scattering of the incident photon with a degraded energy and a deflection angle and transferring energy to an electron in the collision) which is the essential reactions in human tissue for photons in the field of energy which we are concerned in this book. We are able to assess the probability with which this interaction will raise in the sensitive volume and the mean energy transferred to the electron of the sensitive volume (effective and classical physics section). Depending on the size of the sensitive volume, we can also estimate the mean number of interactions therein. However, when these interactions take place, we are unable to determine precisely where this interaction will occur in the sensitive volume, nor with what angle will be emitted secondary electrons set in motion. Consequently, it is impossible to determine the energy imparted ε, by the latter, in the sensitive volume, since we cannot know exactly the track that this emerging electron will perform in this sensitive volume. At this stage, the calculation of the dose is therefore not possible. However, the physical quantity available in this configuration is the energy transferred to the secondary particle that is at the origin of a dedicated quantity to indirectly ionizing radiation (photons and neutrons): it is the "Kerma" which is defined by the ratio of the total energy transferred to the secondary particles into a mass m by the same mass (1.16).

$$\overline{K} = \frac{\overline{E}_{tr}}{m} \tag{1.16}$$

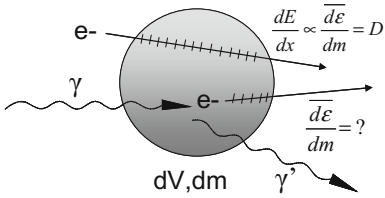

Fig. 1.6 Scheme of the distinction between energy imparted and energy transferred

This quantity is not appropriated for stochastic and a macroscopic context. His unit Gy remains as homogeneous to J kg^{-1}. Like the absorbed dose calculated with (1.10) we obtain the "kerma" by setting the mass m to a negligible amount (1.17).

$$K = \lim_{m \to 0} \overline{K} = \frac{\overline{dE_{tr}}}{dm} \tag{1.17}$$

As the absorbed dose, a kerma rate is defined according (1.18).

$$\dot{K} = \frac{dK}{dt} \tag{1.18}$$

Its unit is the same as the absorbed dose rate, the Gy s^{-1}. To illustrate the conceptual distinction between both fundamental dosimetric quantities that are kerma and absorbed dose, Troesh and Choudens [7] propose a count of energies transferred and imparted in Fig. 1.7.

Consider a mass of infinitesimal element m. In the proposed case in this figure, all of the kinetic energies of the secondary charged particles—electrons—transferred by photon radiation, that is to say the term E_{tr} kerma, is: $E_{tr} = E_1 + E_2$. However, the energy imparted into m, ε allowing access to the calculation of the

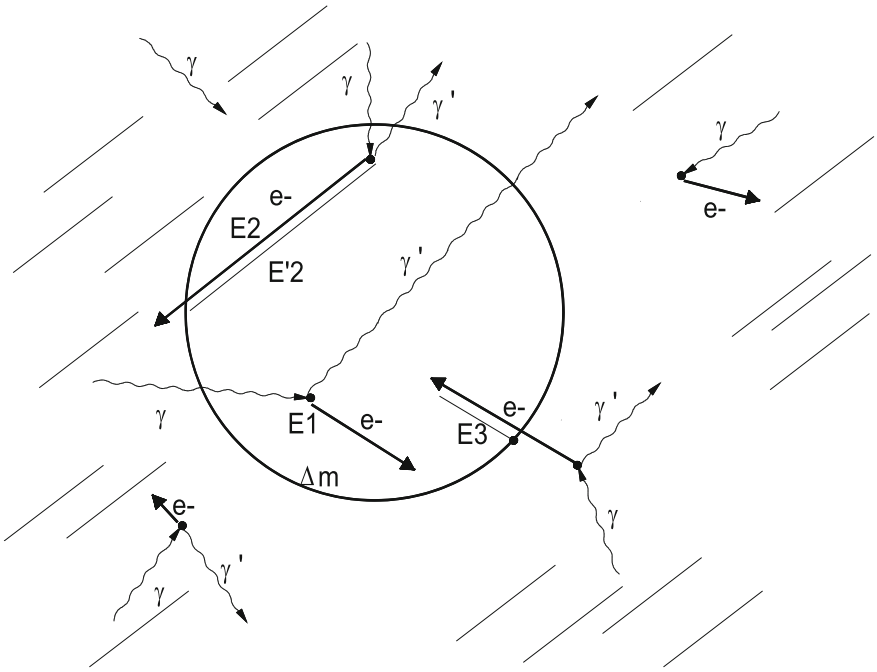

Fig. 1.7 Scheme of the distinction between absorbed dose and kerma in elementary volume, [7]. © Technical Documentation and 1997

absorbed dose is equal to: $\varepsilon = E_1 + E_2' + E_3$. It finally comes $E_{tr} \neq E_{at}$ and therefore for the same elementary mass element m : $D \neq K$. However, we will show in Chap. 2 that under certain conditions and assumptions (equilibrium of secondary charged particles set in motion), equivalence between kerma and absorbed dose for indirectly ionizing radiation is possible. Finally, let's add that the kerma is systematically measurable, while the absorbed dose is so only measurable under certain conditions.

1.2 Biological Damage and Relative Biological Effectiveness (RBE)

1.2.1 Radiation Injury on DNA of the Cell

Upon exposure to directly or indirectly ionizing radiation the cells are impacted and in particular the element most radioreactive thereof: the nucleus and its DNA molecule. The DNA damage may be caused either directly, that is to say, by ionization of the molecule by the passage of the ionizing radiation, or indirectly following a chemical interaction with a free radical produced by irradiation. A radical is a very reactive molecule with a non-bet valence electron. A free radical is a wandering radical which has not yet reacted and thereby threatening its neighbors. Their lifetime is about 10^{-5} s. For example, the ionization of a water molecule will create after several successive chemical reactions, the radical OH (hydroxyl radical) highly reactive, able to damage the DNA molecule in its vicinity. This indirect action via radicals, is the dominant mechanism of damage for low LET radiation, like X-rays.

The human body is composed of 70% water, so most of the damage will raise via OH radical. This justifies the widespread use of water as a irradiated medium in radiobiology studies. Radiation-induced lesions in the DNA consecutive to exposure are of several types: single break or double-stranded DNA-protein bypass formation. Figure 1.8 illustrates the different possible DNA damages by direct and indirect effect.

Among all of these lesions, double-strand breaks are considered as the major responsible for cell inactivation.

Repair mechanisms are triggered by these types of attacks; elimination by excising the lesion and restoration of the original information by resynthesis. However, in some circumstances, they are ineffective against the alteration of the cell structure.

The effects of radiation depend on the spatial distribution of energy deposited in the cell (LET). If the number of fractures formed in a small area of the molecule increases, these cracks can form complexes damage difficult to repair by the cell.

The results of there ineffective repair mechanisms, and chromosomal aberrations it can cause, lead to two outcomes for injured cell: the genetic mutation or death.

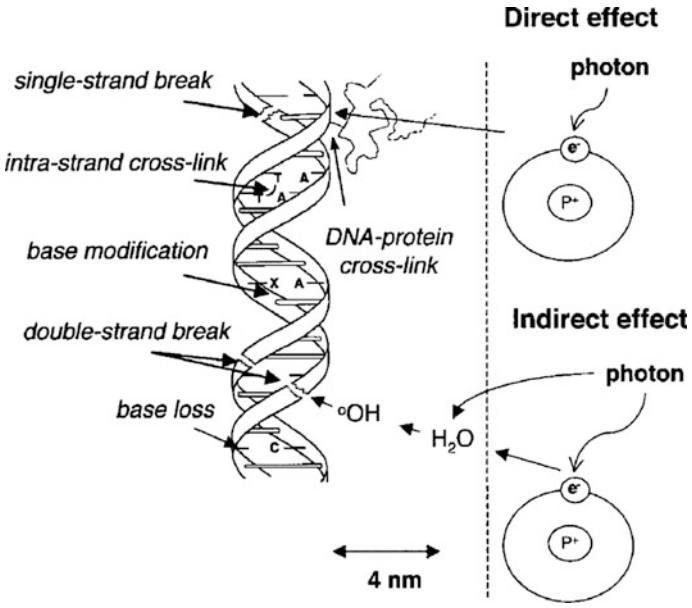

Fig. 1.8 Radiation-induced damage by direct and indirect effect of ionizing radiation on DNA, according to [1], with permission from Springer Heidelberg

Note that this inability is increased when the dose, instead of being spread over time, is instantly distributed; the repair mechanism is then "Swamped". This nuance is essential on the concept of dose rate. Adding that this issue becomes an asset when the aim is to destroy cancer cells: it is entirely appropriate in this context, to deliver a maximum dose in a short time at the tumor to kill most tumor cells as possible.

1.2.2 Cell Survival Rate and RBE

One way to characterize the "dose-effect" at the cellular level is for a given cell type, to observe the cell survival rate in accordance with the increase of the dose. To compare this effect for different types of radiation, radiation biologists have defined "relative biological effectiveness" RBE, which is defined as the ratio between the dose of a reference radiation and studied radiation inducing the same effect, that is to say the cell survival rate S_u. The reference radiation for which the RBE is arbitrarily set to 1 is an X-radiation of 250 keV, 1 MeV gamma, and an absorbed dose rate of 0.1 Gy.min^{-1}. The exposure rate is also important in quantifying biological damage, but we will not go into that level of detail. For any radiation R_i and a cell survival rate S_u, the RBA is calculated according to the expression (1.19).

$$\mathrm{RBE} = \frac{\mathrm{D}(\mathrm{S_u}, \mathrm{X}(250\ \mathrm{keV})}{\mathrm{D}(\mathrm{S_u}, \mathrm{R_i})} \tag{1.19}$$

For example, Fig. 1.9 gives a representation of the cell survival rate for gamma and neutrons.

In Fig. 1.9, to a cell survival rate of 0.1, the RBE obtained according to the expression (1.19) is:

$$\mathrm{RBE} = \frac{\mathrm{D}(0.1; \mathrm{X}(250\ \mathrm{keV})}{\mathrm{D}(0.1; \mathrm{n}[\mathrm{d}(50) + \mathrm{Be}])} = \frac{7.5\ \mathrm{Gy}}{3.8\ \mathrm{Gy}} \cong 2$$

1. 2.5 MeV alpha (Curve 1—LET = 166 keV μm^{-1})
2. 4 MeV alpha (Curve 2—LET = 110 keV μm^{-1})
3. 5.1 MeV alpha (Curve 3—LET = 88 keV μm^{-1})
4. 8.3 MeV alpha (Curve 4—LET = 61 keV μm^{-1})
5. 26 MeV alpha (Curve 5—LET = 25 keV μm^{-1})
6. 3 MeV deuteron (Curve 6—LET = 20 keV μm^{-1})
7. 14.9 MeV deuterons (Curve 7—LET = 5.6 keV μm^{-1})
8. 250 kVp X-rays (Curve 8—LET ≈ 1.3 keV μm^{-1}).

As mentioned above, the damage caused by ionizing radiation leading to cell death are related to the distribution of energy deposition in the cell and thus, for the same dose deposited at LET radiation considered. Figure 1.10 gives a

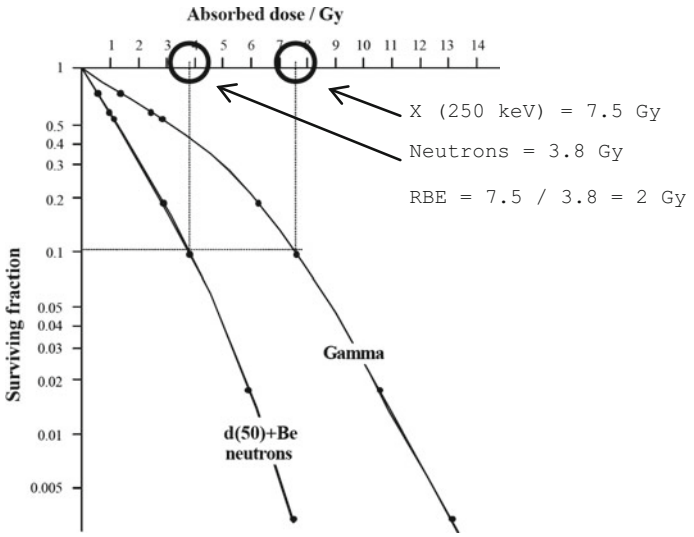

Fig. 1.9 Cell survival rate depending on the dose of gammas and neutrons from the reaction of 50 MeV deuteron on beryllium target—sample calculation RBE, adapted from [8]

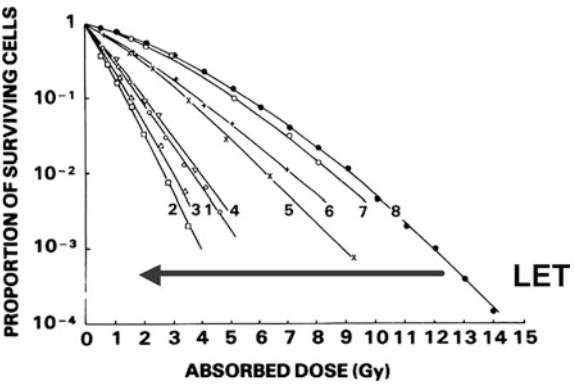

Fig. 1.10 Effect of LET on cell survival curves. Cell survival curves in vitro for human kidney cells exposed to different types of radiation, adapted from [9]

representation of the cell survival rates for renal cells, for different types of decreasing LET radiation.

1. 2.5 MeV alpha (Curve 1—LET = 166 keV μm^{-1})
2. 4 MeV alpha (Curve 2—LET = 110 keV μm^{-1})
3. 5.1 MeV alpha (Curve 3—LET = 88 keV μm^{-1})
4. 8.3 MeV alpha (Curve 4—LET = 61 keV μm^{-1})
5. 26 MeV alpha (Curve 5—LET = 25 keV μm^{-1})
6. 3 MeV deuteron (Curve 6—LET = 20 keV μm^{-1})
7. 14.9 MeV deuterons (Curve 7—LET = 5.6 keV μm^{-1})
8. 250 kVp X-Rays (Curve 8—LET ≈ 1.3 keV μm^{-1}).

Note that the RBE increases with the increase of LET (since the deposited dose required for the same effect decreases [denominator (1.19)]. However, this applies to a LET about 110 keV $\mu m\ m^{-1}$ (curve 2, 4 MeV alpha), beyond the RBE decreases (curve 1, 2.5 MeV alpha). Figure 1.11 gives the RBE as a function of LET microscopic equivalent: the lineal energy y. From it are determined "transfer factors" needed to obtain protection and operational quantities, respectively the weighting factor for radiation w_R and the quality factor Q we will detail later in Chap. 3.

We can admit that a cell is killed when it has accumulated a certain amount of damage. Consider this occurrence takes place arbitrarily when three ionization takes place (ionization = black dots). The three configurations of the illustration proposed in Fig. 1.12 are lethal to the cell.

Configuration (1). For low LET radiation, below 15 keV μm^{-1}, the amount of energy deposition (and thus damage) by passing a weak trajectory is generally to cause cell death and more paths are required to accumulate enough damage and kill the cell. The amount of energy increases with LET and it takes less track to kill the cell, it results in an increase of the RBE between 15 keV μm^{-1} and up to about 50 keV μm^{-1}.

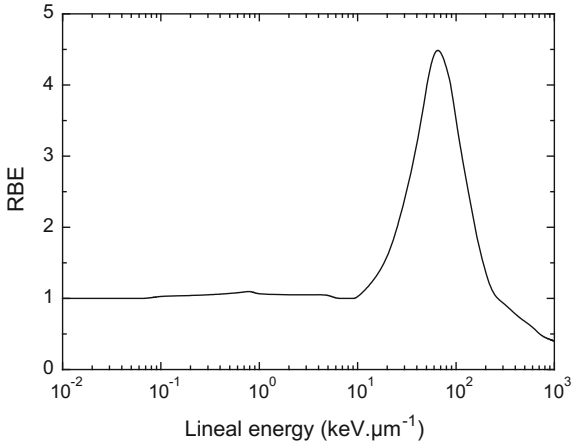

Fig. 1.11 Relative biological effectiveness (RBE) based on the lineal energy, adapted from [10]

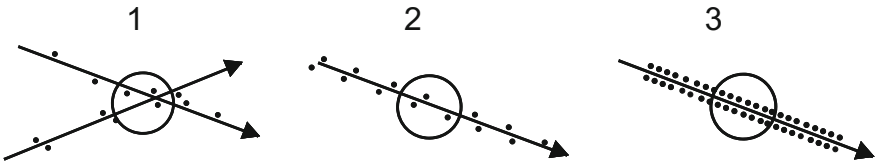

Fig. 1.12 Diagram of three lethal configurations for the cell—black dots are the successive ionization along the path, according to [8]

Configuration (2). RBE maximum is reached when a single path delivers on average just enough energy to kill the cell between 50 and 100 keV μm^{-1}.

Configuration (3). Beyond, the passage of a single path expends more energy than necessary to kill the cell, there is a "waste of energy" and in fact decrease the RBE since the definition is the ratio of doses required to produce a given effect. Furthermore, with a massive energy deposition over a short distance, the following cells will be made more "spared" at equal dose than in the case of particles with lower LET; we speak of an "energy cluster" effect.

Figure 1.13 adds to this RBE microdosimetric curves, spectra of three types of particles: gamma, protons and neutrons.

Strictly speaking, with a LET $\overline{L}$ approach, the RBE value is partially incorrect. In particular, as shown in Fig. 1.13 for the interval of microdosimetric spectrum located in the region of strongest RBE: 50 and 100 keV μm^{-1}. The method of calculation of the mean RBE incorporates this strong RBE area. if $r(y)$ is RBE

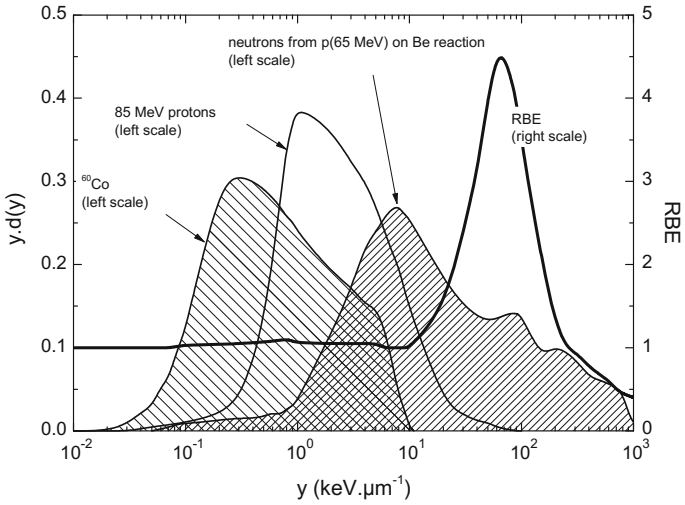

Fig. 1.13 Curve RBE and microdosimetric spectra gamma ^{60}Co, 85 MeV proton and neutron from the bombardment of a beryllium target with protons of 65 MeV, adapted from [10]

in respect with given lineal energy, mean EBR is calculated using the expression (1.20).

$$\overline{\mathrm{EBR}} = \int_{y_{min}}^{y_{max}} r(y)\, d(y)\, dy \tag{1.20}$$

It is recalled that the dose distribution in the lineal energy $d(y)$ is normalized to 1 (see Further Details 1.1). We will see in Chap. 2 that is with mean of this approach that is calculated the mean quality factor for a radiation field.

1.3 Radiometric Quantities

Dosimetric quantities of reference, punctual concepts, are absorbed dose D and Kerma K respectively defined by the expression (1.10) and (1.17). In the above, we have clearly established link between these specific quantities and ionizing radiation density in the sensitive volume. We therefore propose in this part to define the physical quantities to characterize directly and indirectly ionizing radiation field, called "radiometric quantities." From some of them, it will be possible to assess the dose quantities previously described.

1.3.1 Radiation Field Characterization

To determine at point P in space the action of radiation in a given environment, we define the radiation field characterized by the mathematical function to six variables: $\varphi_u\left(\vec{r},\vec{u},E,t\right)$. This function is the number of particles propagating at a point P of the spatial coordinate $\vec{r}$, in the direction $\vec{u}$, In a solid angle Ω, around $\vec{u}$, with an energy E, at time t according to the diagram of Fig. 1.14. This is called "angular distribution of fluence."

In Cartesian coordinates, the unit vector $\vec{u}$ is defined by (1.21).

$$\vec{u}\begin{cases}\sin\theta\cdot\cos\varphi\\ \sin\theta\cdot\sin\varphi\\ \cos\theta\end{cases} \tag{1.21}$$

Prior to the practical definition of this quantity, it should define a number of tools and intermediate quantities.

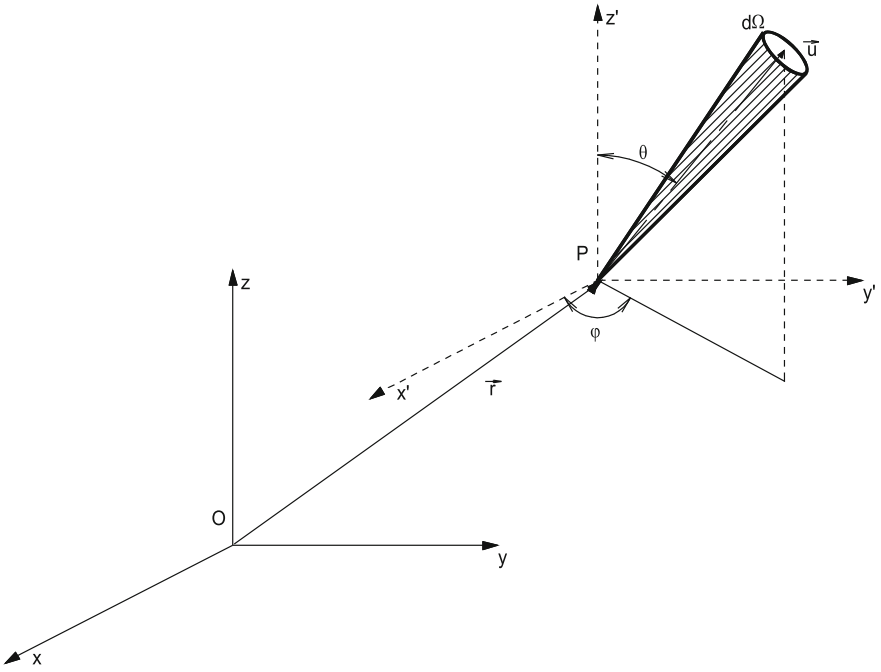

Fig. 1.14 Representation of an angular distribution of fluence

1.3.2 Radiant Energy and Flux

The number of particles emitted transferred or received at a point is characterized by the variable N (Dimensionless). The "radiant energy R" is defined as the total energy of the particles (excluding the rest energy) transferred or received in a point; his unit is the joule. To illustrate these terms, consider that a point in space, cross N particles and that they have 4 discrete possible energies: E_1, E_2, E_3 or E_4. We can then represent "the energy distribution" of these N particles according to Fig. 1.15.

The number of particles N is the sum of all the particles, regardless of their energy, and is given by (1.22). The radiant energy R also a sum, but this time the number of particles N *is* weighted by respective energy *Ei* (1.23).

$$\mathrm{N} = \sum_{\mathrm{i}} \mathrm{N}(\mathrm{E_i}) \tag{1.22}$$

$$\mathrm{R} = \sum_{\mathrm{i}} \mathrm{N}(\mathrm{E_i}) \cdot \mathrm{E_i} \tag{1.23}$$

We can then calculate a weighted average of the mean energy this energy distribution according (1.24).

$$\overline{E} = \frac{R}{N} = \frac{\sum_i N(E_i) \cdot E_i}{\sum_i N(E_i)} \tag{1.24}$$

In the case of 4 rays emission, shown in Fig. 1.15, the ratio of the radiant energy by the number of particles emitted, leading to the result of the mean energy would be:

$$\overline{E} = \frac{R}{N} = \frac{N_1E_1 + N_2E_2 + N_3E_3 + N_4E_4}{N_1 + N_2 + N_3 + N_4}$$

While this trivial approach is applicable, for example, de-excitation photons emitted during radioactive decay, most distributions encountered in the nuclear environment (particle accelerator, reactors, cosmic …) are continuous. More readily we speak of "spectral energy distribution" or "energy spectra."

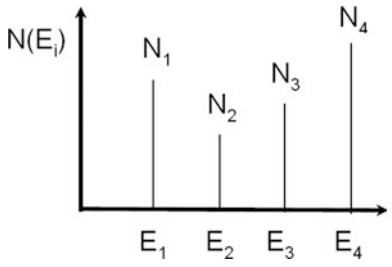

Fig. 1.15 Example of discrete energy distribution

In the context of continuous distribution, if N is the number of particles passing through a point in space whose energy distribution is continuous, it is necessary to define "the spectral energy distribution" characterized by the ratio of the increase in the number dN in the energy interval between infinitesimal E and E + dE (1.25).

$$\mathrm{N_E} = \left(\frac{\mathrm{dN}}{\mathrm{dE}}\right) \tag{1.25}$$

This variable dimension is an inverse of energy: keV^{-1} or MeV^{-1}. Thus, in this continuous distribution context, the term (1.23) becomes (1.26).

$$\mathrm{R} = \int_0^{\mathrm{E_{Max}}} \left(\frac{\mathrm{dN}}{\mathrm{dE}}\right) \mathrm{E}\,\mathrm{dE} = \int_0^{\mathrm{E_{Max}}} \mathrm{N_E E}\,\mathrm{dE} \tag{1.26}$$

Similarly, the mean energy obtained previously by the expression (1.24) is obtained by this time (1.27).

$$\overline{\mathrm{E}} = \frac{\int_0^{\mathrm{E_{Max}}} \mathrm{N_E E}\,\mathrm{dE}}{\int_0^{\mathrm{E_{Max}}} \mathrm{N_E}\,\mathrm{dE}} \tag{1.27}$$

In order to integrate the time component, we define the "flux" or "emission" in the case of a source that emits N particles per unit time according (1.28).

$$\dot{\mathrm{N}} = \left(\frac{\mathrm{dN}}{\mathrm{dt}}\right) = \lim_{\mathrm{t}\to 0}\left(\frac{\mathrm{N}}{\mathrm{t}}\right) \tag{1.28}$$

The size of this variable is (s^{-1}). In the literature, particularly in the standards, this variable is sometimes symbolized by *B (for Beam)*. We will actually not difficult to be convinced of the similarity there may be between a point source which emits radiation with a certain flux $\dot{N}$ and a point in space crossed with a flux $\dot{N}$. If both situations are not physically the same, the quantity that characterizes the number of radiation emerging at a time t is the same in both cases: $\dot{N}$.

Finally, note that there is also the quantity "radiant energy flux" $\dot{R}$, according to (1.29).

$$\dot{\mathrm{R}} = \left(\frac{\mathrm{dR}}{\mathrm{dt}}\right) \tag{1.29}$$

This quantity is the ratio of increase of the radiant energy R over a time interval t in a point of space. Its unit is typically the MeV s^{-1}. We have just defined punctual radiometric quantities applicable to continuous spectral distributions. In practice, the lack of analytical expression or precision in the experimental

information requires treating the representations of these quantities by histograms of energy bins and performing a sampling of the energy distribution.

If $\dot{N}$ is particles flux in a point in space whose energy distribution is continuous, it is necessary to define the spectral energy distribution characterized by the ratio of the increase in transmission the source $d\dot{N}$ in the energy interval between infinitesimal E and $E + dE$ (1.30).

$$\dot{N}_E = \left(\frac{d\dot{N}}{dE}\right) \tag{1.30}$$

This variable has the typical size: $MeV^{-1}\ s^{-1}$. This distribution is used to determine the part of emission or particle flux within the energy range between E_1 and E_2 according to (1.31), as shown in Fig. 1.16.

$$\dot{N}(E_1; E_2) = \int_{E_1}^{E_2} \dot{N}_E \, dE \tag{1.31}$$

Indeed, across the spectrum, we get the total value of particle flux (1.32)

$$\dot{N} = \int_0^{E_{Max}} \dot{N}_E \, dE \tag{1.32}$$

As a simple example, consider the spectral distribution characteristic of the source emission or a flux of 1000 (n) s^{-1} whose energy is between 1 and 10 MeV. This is thus defined by:

$$\begin{aligned} \dot{N}_E &= 1000/10 = 100\ MeV^{-1}\ s^{-1} \quad E \in [1\ MeV;10\ MeV] \\ \dot{N}_E &= 0 \qquad\qquad\qquad\qquad\qquad\quad E \notin [1\ MeV;10\ MeV] \end{aligned}$$

that may be represented by Fig. 1.17.

In some very rare cases, it is possible to assess the analytical expression, true or approaching, the spectral energy distribution of the emission of a source or a stream of particles. For example, this is the case for the neutron emission by spontaneous fission,

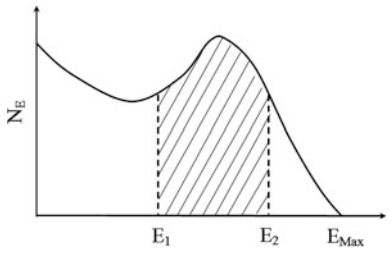

Fig. 1.16 Spectral energy distribution of a source emission or a particle flux for a continuous distribution

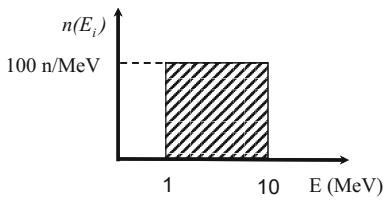

Fig. 1.17 Energy distribution of a flux of 1000 (n) s^{-1}, the neutron energy is between 1 and 10 MeV

as will be illustrated later in this paragraph by the spontaneous fission spectrum of ^{252}Cf radionuclide.

1.3.3 Application to Neutron Spectrum of ^{252}Cf

The probability that a neutron is emitted with an energy E during fission is described by an analytical expression of type "Maxwell" (1.33).

$$\mathrm{p(E)} = \frac{2}{\sqrt{\pi}\mathrm{T}^{3/2}}\left(\sqrt{\mathrm{E}}\right)\exp\left(-\frac{\mathrm{E}}{\mathrm{T}}\right) \tag{1.33}$$

With T a parameter of the spectrum (T = 1.42 MeV for the ^{252}Cf [11]). The spectral distribution by weighting this probability density by issuing $\dot{N}$ Source is accessed (1.34).

$$\dot{N}_E = p(E)\dot{N} \tag{1.34}$$

For example, let's determine the emission rate of 0.6 MeV neutron by a ^{252}Cf source for a total neutron emission $\dot{N}$ normalized to 1(n) s^{-1}.

$$\dot{N}_{0.6} = p(0.6)\dot{N} = \frac{2}{\sqrt{\pi}(1.42)^{3/2}}\left(\sqrt{0.6}\right)\exp\left(-\frac{0.6}{1.42}\right) \times 1 = 0.338\ \mathrm{s}^{-1}$$

In what follows, we describe how are represented practically the data of this type of energy distribution, first in a table and then graphically.

1.3.4 Representation of Data to an Energy Distribution in an Array

In Table 1.2, The spectral energy distribution is given in the form of groups $\dot{N}_i$ according to energy bins, meaning that the emission of neutrons having an energy between E_i and E_{i+1} is obtained according to (1.35).

Table 1.2 Example of an energy bin distribution for the ^{252}Cf source [11] data from NF ISO 8529-1 March 2002 © AFNOR 2002

Ei (MeV)	N_i (s^{-1})	Ei (MeV)	N_i (s^{-1})	Ei (MeV)	N_i (s^{-1})	Ei (MeV)	N_i (s^{-1})
4.14×10^{-7}	3.10×10^{-10}	4.00×10^{-2}	2.80×10^{-3}	6.00×10^{-1}	3.38×10^{-2}	3.50×10^{0}	4.68×10^{-2}
1.00×10^{-6}	1.11×10^{-8}	6.00×10^{-2}	3.29×10^{-3}	7.00×10^{-1}	3.39×10^{-2}	4.00×10^{0}	3.49×10^{-2}
1.00×10^{-5}	2.76×10^{-7}	8.00×10^{-2}	3.68×10^{-3}	8.00×10^{-1}	3.37×10^{-2}	4.50×10^{0}	2.58×10^{-2}
5.00×10^{-5}	2.76×10^{-7}	1.00×10^{-1}	1.05×10^{-2}	9.00×10^{-1}	3.33×10^{-2}	5.00×10^{0}	3.30×10^{-2}
1.00×10^{-4}	7.82×10^{-7}	1.50×10^{-1}	1.21×10^{-2}	1.00×10^{0}	6.46×10^{-2}	6.00×10^{0}	1.74×10^{-2}
2.00×10^{-4}	2.21×10^{-6}	2.00×10^{-1}	1.33×10^{-2}	1.20×10^{0}	6.12×10^{-2}	7.00×10^{0}	9.01×10^{-3}
4.00×10^{-4}	4.53×10^{-6}	2.50×10^{-1}	1.42×10^{-2}	1.40×10^{0}	5.73×10^{-2}	8.00×10^{0}	4.61×10^{-3}
7.00×10^{-4}	5.68×10^{-6}	3.00×10^{-1}	1.49×10^{-2}	1.60×10^{0}	5.31×10^{-2}	9.00×10^{0}	2.33×10^{-3}
1.00×10^{-3}	5.51×10^{-5}	3.50×10^{-1}	1.55×10^{-2}	1.80×10^{0}	4.88×10^{-2}	1.00×10^{1}	1.17×10^{-3}
3.00×10^{-3}	1.28×10^{-4}	4.00×10^{-1}	1.60×10^{-2}	2.00×10^{0}	6.55×10^{-2}	1.10×10^{1}	5.83×10^{-4}
6.00×10^{-3}	2.30×10^{-4}	4.50×10^{-1}	1.63×10^{-2}	2.30×10^{0}	5.67×10^{-2}	1.20×10^{1}	2.88×10^{-4}
1.00×10^{-2}	7.74×10^{-4}	5.00×10^{-1}	1.66×10^{-2}	2.60×10^{0}	6.33×10^{-2}	1.30×10^{1}	1.42×10^{-4}
2.00×10^{-2}	2.17×10^{-3}	5.50×10^{-1}	1.68×10^{-2}	3.00×10^{0}	6.21×10^{-2}	1.40×10^{1}	6.94×10^{-5}
						1.50×10^{1}	–

$$\dot{\mathrm{N}}_{\mathrm{i}} = \int_{\mathrm{E_i}}^{\mathrm{E_{i+1}}} \dot{\mathrm{N}}_{\mathrm{E}}\, \mathrm{dE} \tag{1.35}$$

In this case of the spontaneous fission emission of the ^{252}Cf source, $\dot{N}_i$ groups are calculated by numerical integration using the analytic function (1.34). For other sources—e.g. ^{241}Am (α, n)Be—this type of expression is not accessible and experimental data are used. More generally, for any flux particles, at a point in space, process would be the same; accessed by measurement or by numerical simulation (e.g. type of transport code Monte Carlo) with results by energy bins. In Table 1.2, the energy given to each $\dot{N}_i$ is the lower limit, *Ei* of the energy interval index *i*, the last energy index specified in each table is the upper limit of the last energy interval index. In the case of Table 1.2, energy bins are normalized to a total emission: $\dot{N}_i = 1\ \mathrm{s}^{-1}$. The sum leads to unity (1.36).

$$\sum_{\mathrm{i=1}}^{\mathrm{n}} \dot{\mathrm{N}}_{\mathrm{i}} = 1\ \mathrm{s}^{-1} \tag{1.36}$$

For example, to calculate the flux part of the 25th energy bin in Table 1.2 (the lower bound *Ei* = 0.6 MeV), the numerical calculation leads to the result in accordance with that announced by Table 1.2.

$$\dot{N}_{25} = \int_{0.6}^{0.7} \frac{2}{\sqrt{\pi}(1.42)^{3/2}} \left(\sqrt{E}\right) \exp\left(-\frac{E}{1.42}\right) dE \cong 0.038\ \mathrm{s}^{-1}$$

The values given in the table allow to calculate the flux part between the energies E_a and E_b by simply adding the corresponding emission groups (1.37).

$$\dot{N}(E_a; E_b) = \sum_{i=a}^{i=b-1} \dot{N}_i \tag{1.37}$$

Note that this expression is a "sampled" approach to the expression of a continuous distribution (1.31).

Thus, to know the ^{252}Cf neutron emission between 0.6 and 1.2 MeV: 25th group (i.e. lower bound *Ei* = 0.6 MeV) up to 29th group (i.e. lower bound *Ei* = 1 MeV), the sum (1.37) with the values in Table 1.2 gives:

$$\dot{\mathrm{N}}(0.6; 1.2) = \sum_{\mathrm{i=25}}^{\mathrm{i=29}} \dot{\mathrm{N}}_{\mathrm{i}} \approx 0.2\ \mathrm{s}^{-1}$$

Obtaining the mean energy of the spectral energy distribution of this "histogram approach", while the expression (1.27) for the continuous approach, is obtained according to (1.38).

$$\bar{E} = \frac{\sum_{i=1}^{n} \dot{N}_i \, E_i}{\sum_{i=1}^{n} \dot{N}_i} \tag{1.38}$$

In the case of normalization, in Table 1.2, the previous expression becomes (1.39) and we obtained for ^{252}Cf:

$$\bar{E}\left(^{252}Cf\right) = \sum_{i=1}^{n} \dot{N}_i E_i \approx 2.13 \text{ MeV} \tag{1.39}$$

The size of flux intervals necessarily influences the value of the mean energy and its deviation from its true value.

1.3.5 Graphical Representation Distribution Energy

While the values of flux bins are the fundamental data from physical measurements or calculations and serving in other integration calculations, they are inappropriate for the graphic representation of the spectra because their values depend on the width (arbitrary) energy intervals. For sources, the most common graphic representations are the spectral emission $\dot{N}_E = \mathrm{d}\dot{N}/\mathrm{d}E$ in terms of E when the energy is in linear scale and represented by (1.40) when E is a logarithmic scale.

$$\frac{d\dot{N}}{d(\ln(E/E_o))} \tag{1.40}$$

Historically this term comes from the neutron and is known as "plotted lethargy". Arbitrary parameter E_0 is necessary to ensure that the argument of the logarithm is of dimension 1, and mathematically as: d(ln x) = dx/x. It results from the equality (1.41).

$$\frac{\mathrm{d}\dot{N}}{\mathrm{d}(\ln(E/E_o))} = E\left(\frac{\mathrm{d}\dot{N}}{\mathrm{d}E}\right) = E\dot{N}_E \tag{1.41}$$

So for energy, x-axis, expressed in logarithmic scale, it will be common to see one of the three formalisms equality (1.41). Based on these assumptions, it is possible to draw curves so that equal areas under the curves represent equal particle flux.

$$\int_{E_1}^{E_2} \dot{N}_E \, \mathrm{d}E = \int_{E_1}^{E_2} E\dot{N}_E (\mathrm{d}E/E)$$

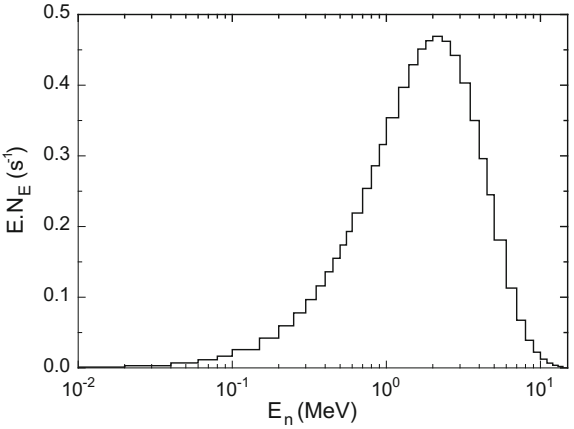

Fig. 1.18 Energy distribution of spontaneous fission neutron emission for ^{252}Cf with the graduated abscissa in logarithmic scale, from Table 1.2

Note that $E\dot{N}_E$ has again the dimension of a particle flux (s^{-1}), while a curve with graduated abscissa linearly, the ordinates of values would be calculated from the approach "sampled" by (1.42).

$$\dot{N}_E = \frac{\Delta\dot{N}}{\Delta E} = \frac{\dot{N}}{(E_{i+1} - E_i)} \tag{1.42}$$

They must be for a plot with the graduated abscissa logarithmically calculated according to (1.43).

$$E_n\dot{N}_E = \frac{\dot{N}_i}{\ln(E_{i+1}/E_i)} \tag{1.43}$$

Let us add that because of spectra that can be spread over ten decades logarithmic representation is required. Figure 1.18 gives a product of the histogram $E\dot{N}_E$ of ^{252}Cf on a linear axis, as a function of neutron energy *En* on a logarithmic x-axis.

1.3.6 Fluence Definition and Interest in Dosimetry and Radiation Protection

The question we can ask at this stage is: the particle flux $\dot{N}$ at a point of the space it is sufficient to characterize the radiation field and, consequently, the absorbed dose at a point? The answer is no. We have been clear, in previous paragraphs that the greater the spatial density of radiation is important for a same time interval and the absorbed dose or kerma increased. If we consider two sensitive sites with slightly different volumes, crossed by three radiations, the flux of particles in these two sites

is the same: $\dot{N}_1 = \dot{N}_2$. Volumes are different however: this necessarily leads to an absorbed dose or kerma in the case of indirectly ionizing radiation, different in both cases (Fig. 1.19).

In addition to increasing the amount of radiation which passes through a point in space during the time interval we are obliged to use a variable that takes into account the spatial density of radiation. This quantity is called "fluence". We can for example characterize it considering a microscopic sphere of radius r, Volume V and section a (area describing the boundary between the two half-spheres) and counting the radiation which pass through the section a as shown in Fig. 1.20.

There is a simple calculation method, which is also used in the Monte Carlo transport code, to achieve this radiant quantity. The latter is to recognize all radiation entering the volume of sphere V and radius r and to weight the latter by the mean length of chord, while dividing the final result by the volume V. If N is the number of particles counted, the "mean fluence" in Volume V is then described by the expression (1.44)

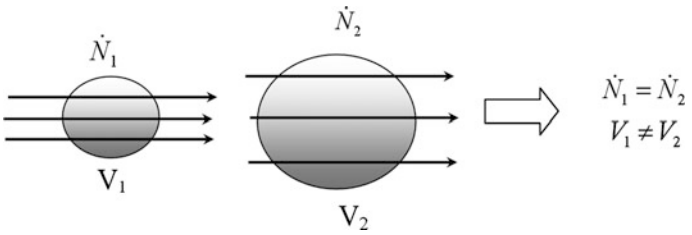

Fig. 1.19 Illustration of use limit of flux for an application in dosimetry and radiation protection

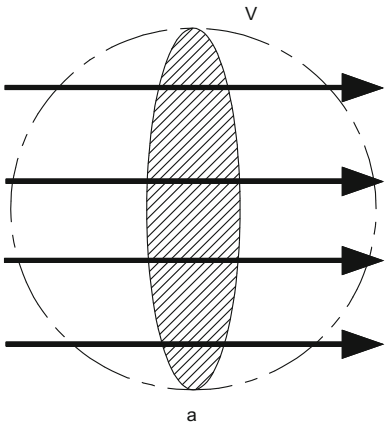

Fig. 1.20 Illustration of the fluence calculation in a sensitive site comparable to a sphere of radius r and section a

$$\bar{\Phi} = \frac{N\bar{l}}{V} \tag{1.44}$$

This is a mean result; we assumes indeed that on average, an incoming particle performs in Volume V a path length equal to the mean chord. Knowing the value of the previously calculated mean chord ($\bar{l} = (4/3)r$). In the case of a sensitive volume theoretically materialized by a sphere, we deduce a trivial result for expression (1.45).

$$\bar{\Phi} = \frac{N(4/3)r}{(4/3)\pi r^3} = \frac{N}{\pi r^2} = \frac{N}{a} \tag{1.45}$$

This amounts to counting the number of particles that cross the section (a) of the sphere. The practical unit of this quantity is cm^{-2}. From this mean microscopic quantity, it comes to getting a punctual quantity that can be connected to punctual dose quantities previously defined. This is achieved by setting the section to a negligible amount, according to (1.46).

$$\lim_{a\to 0} \bar{\Phi} = \frac{dN}{da} = \Phi \tag{1.46}$$

This quantity is called "particle fluence at a point in space" and is linked to most dose quantities and radiation related to external exposure. From this quantity, we define a "fluence rate" according (1.47).

$$\dot{\Phi} = \frac{d\Phi}{dt} \tag{1.47}$$

His unit is $cm^{-2}\ s^{-1}$. Thus, with the knowledge of the energy of radiation and of this quantity, all data are now available to characterize the radiation field at a point in space from which it is possible to obtain fundamental dosimetric quantities by means of a correlation coefficient. Below, from the fluence and with the knowledge of the energy of the incident radiation (for simplicity, we consider here only one possible energy E). It will be possible to determine the absorbed dose and kerma by simple proportionality relationship (1.48).

$$\begin{cases} K = k_\Phi(E)\Phi(E) \\ D = d_\Phi(E)\Phi(E) \end{cases} \tag{1.48}$$

The challenge in Chap. 2 will consist of determining precisely these correlation coefficients, with the knowledge of the energy transfer phenomena during the interaction of different types of radiation with matter.

As with the particle flux for a continuous spectrum, it is possible to define a spectral distribution of the fluence called "differential energy fluence" and

translating increasing fluence Φ on a range of the spectrum between energies E and $E + dE$ (1.49).

$$\Phi_E = \frac{d\Phi}{dE} \tag{1.49}$$

Its typical unit is cm^{-2} MeV^{-1}. As before, for the contribution to the total fluence Φ to an energy interval between E_1 and E_2. Calculation is performed according (1.50).

$$\Phi(E_1; E_2) = \int_{E_1}^{E_2} \Phi_E dE \tag{1.50}$$

Again, by integrating over the full spectrum, we obtain complete fluence Φ for the radiation field at the point considered. Another variable is likely to interest dosimetry, it is the "energy fluence" used to summon the energies of N particles that cross section *at* of Fig. 1.20. It is expressed in infinitesimal manner from the radiant energy and differential energy fluence as expressed in (1.51).

$$\Psi = \frac{dR}{da} = \int_E \left(\frac{d^2N}{da\, dE}\right) EdE = \int_E \Phi_E E\, dE \tag{1.51}$$

His unit is expressed typically in MeV cm^{-2}. We define the "energy fluence rate" in the words (1.52)

$$\dot{\Psi} = \int_E \dot{\Phi}_E E\, dE \tag{1.52}$$

whose unit is expressed in MeV in cm^{-2} s^{-1}. We also calculate these quantities from the mean energy of a radiation spectrum as (1.53).

$$\bar{E} = \frac{\int_0^\infty \Phi_E E\, dE}{\int_0^\infty \Phi_E dE} = \frac{\Psi}{\Phi} \tag{1.53}$$

All that has been previously discussed for the bin setting in the graphical representation of source emission can be applied to the particle fluence. Thus, when the abscissa is set to logarithmic scale, it will be common to read one of the three formalisms given below, for the ordinate of the differential energy fluence Φ_E.

$$\frac{d\Phi}{d(\ln(E/E_o))} = E\left(\frac{d\Phi}{dE}\right) = E\Phi_E \tag{1.54}$$

Let's finally mention two other quantities of interest for isotropic or rotationally symmetrical source (e.g. target irradiated by beam accelerator). The "angular fluence rate" characterize the number of particles spreading in a solid angle Ω during a

time t (1.55) whose unit is the Sr^{-1} s^{-1} and the angular energy fluence rate (1.56), whose unit is the MeV Sr^{-1} s^{-1}.

$$\omega = \frac{d^2N}{dt\, d\Omega} \tag{1.55}$$

$$\omega_E = \frac{d^2R}{dt\, d\Omega} \tag{1.56}$$

Although discrete radiation is encountered in conventional radiation sources: de-excitation photon during decays, conversion electrons, secondary particles of energy secured in the event of special nuclear reactions (e.g. 14 MeV neutron to the fusion reaction) … in most situations shielding, interposition or structural elements of facility affect these discrete energy which results in continuous energy spectrum. We'll develop it extensively in the following chapters. For now, to illustrate how to practice fluence, we propose to study the properties related to the calculation of the fluence induced by isotropic point source, that is to say, emitting the same way in all directions of space.

1.3.7 Calculating the Fluence Induced by an Isotropic Point Source

Let's apply the expression (1.45) of the particles fluence rate in case of an isotropic point source. Beforehand, let's determine by which surface it's necessary to divide the particles flux to get the fluence rate at a distance r from an isotropic source. An isotropic source transmits with equal probability in all directions in space and consequently provide a spherical symmetry for the emission of particles. This property allows to assume that in a virtual sphere centered on the source of radius r_1, each cm^2 of the sphere is crossed by the same number of particles. If we increase the radius to a value r_2, we can intuitively convince us that this property remains true, but in this case the number of particles passing through each cm^2 decrease, since the distance from the source. Figure 1.21 shows schematically this basic concept.

Indeed, one can figure out that three particles emitted by the source spaced from each other with the same angle—because of the spherical symmetry—cross 1 cm^2 of the sphere of radius r_1; because of the path divergence, only one particle pass through 1 cm^2 of the sphere of radius r_2. Thus, to the distance r_1, we have a fluence of three particles per cm^2 and to the distance r_2, a fluence of one particle per cm^2. Thus, the larger the radius of the sphere increases, the lower the fluence rate of particles will be important in a point thereof. The expression of the particle fluence at a distance r of the source in the case of an isotropic source in space is given by the ratio of the number of particles emitted by the source, on the surface of the "virtual" sphere of radius r as expressed by (1.57).

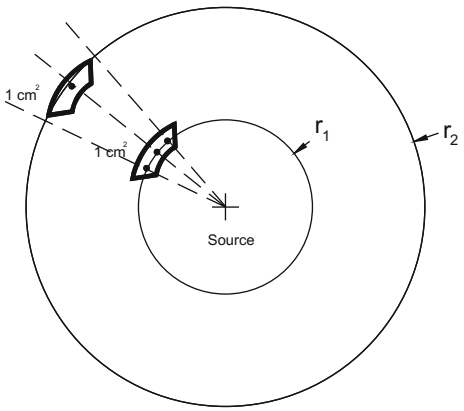

Fig. 1.21 Fluence rate of an isotropic source in space and impact of the distance of calculation point

$$\Phi = \frac{N}{4\pi r^2} \tag{1.57}$$

Note that the fluence can be likened to a spatial density of current flowing through a sphere at a distance r to the source.

By taking up the case of the previous two spheres and a number of particles N, we get the following fluence of particles:

$$\Phi_1 = \frac{N}{4\pi r_1^2} \quad \text{and} \quad \Phi_2 = \frac{N}{4\pi r_2^2}$$

We can spontaneously notice the following property:

$$\frac{\Phi_1}{\Phi_2} = \left(\frac{r_2}{r_1}\right)^2.$$

and yet that:

$$\Phi_1 = \left(\frac{r_2}{r_1}\right)^2 \Phi_2$$

So it is possible to spontaneously get a fluence of particles at any distance from the source, if you know the value of the fluence at another distance. More generally for two distances d_1 and d_2 responsible for respective influences Φ_1 and Φ_2, the relationship between all of these terms is given by (1.58).

$$\frac{\Phi_1}{\Phi_2} = \left(\frac{d_2}{d_1}\right)^2 \tag{1.58}$$

Note, finally, that this law is necessarily valid for the ratio of particle fluence rates:

$$\frac{\dot{\Phi}_1}{\dot{\Phi}_2} = \left(\frac{d_2}{d_1}\right)^2$$

To illustrate concretely some of the variables described below, apply these concepts to simple cases. For example, consider a point source that emits isotropically, $\dot{N} = 5 \cdot 10^6$ particles per second, calculate the angular fluence rate, fluence rate to 1 and 3 m. For this calculation, divide the number of particles emitted per unit of time by the total solid angle around the source, i.e. 4π; we are getting then:

$$\omega = \frac{\dot{N}}{4\pi} = \frac{5 \cdot 10^6}{4\pi} \cong 4 \cdot 10^5 \text{ Sr}^{-1} \text{ s}^{-1}$$

Note that from the angular fluence rate, we can get directly the fluence rate at any distance from the source: it is sufficient to divide ω by the squared distance. Thus we get the fluence rates at 1 and 3 m, as following:

$$\dot{\Phi}_{1\,\text{m}} = \frac{\omega}{d^2} = \frac{N}{4\pi d^2} = \frac{4 \cdot 10^5}{100^2} = 40\,\text{cm}^{-2}\text{s}^{-1} \quad \text{and}$$
$$\dot{\Phi}_{3\,\text{m}} = \frac{\omega}{d^2} = \frac{N}{4\pi d^2} = \frac{4 \cdot 10^5}{300^2} = 4.4\,\text{cm}^{-2}\,\text{s}^{-1}$$

Now consider an isotropic point source in space, whose flux is $3 \cdot 10^5$ particles per second, with isotropic energy and emitting a single energy ray of 0.6 MeV. Calculate the angular energy fluence rate and energy fluence rate at 0.5 m.

$$\omega_E = \frac{\dot{N}E}{4\pi} = \frac{3 \cdot 10^5 \cdot 0.6}{4\pi} = 1.4 \cdot 10^4 \text{ MeV Sr}^{-1} \text{ s}^{-1}$$

was obtained, similarly to previously, the energy fluence rate to 0.5 m:

$$\left(\dot{\Phi}E\right)_{0.5\,\text{m}} = \frac{\omega_E}{d^2} = \frac{NE}{4\pi\, d^2} = \frac{1.4 \cdot 10^4}{50^2} = 5.6\,\text{MeV cm}^{-2}\,\text{s}^{-1}$$

A 1 MBq point source of ^{65}Ni emits through the decay β, 366, 1116 and 1482 keV gamma-rays, respectively with the emission rates: 5, 15 and 24% [12]; we get the energy fluence rate 0.5 m, in the void:

$$\psi_{0.5\,\text{m}} = \frac{A\sum_{i=1}^{3}\Gamma_i E_i}{4\pi\, d^2} = \frac{1 \cdot 10^6 \times (0.366 \times 5 \cdot 10^{-2} + 1.116 \times 0.15 + 1.482 \times 0.24)}{4\pi(50)^2}$$
$$= 17.2 \text{ MeV cm}^{-2} \text{ s}^{-1}$$

1.3.8 Calculation of the Fluence Induced by a No Punctual Source

For non-point object, let it a density of activity corresponding to the ratio of the total activity of the radiating object on length, area or volume depending on the number of dimensions that characterizes it. The calculation of the fluence at a point then is provided by an integration on all the dimensions of the object. This approach physically equivalent to considering the object as a sum of independent point sources.

To illustrate the case of calculating the fluence for a non-point source, consider a linear source of flux $\dot{N}$ and length L. Figure 1.22 represents the studied geometry.

Considering the flux volume density $n_L = \dot{N}/L$, the expression of flux density due to an infinitesimal element "dl" is given by the following expression:

$$d\dot{\Phi} = \frac{n_L}{4\pi\rho^2} dl$$

we have mathematically:

$$\text{h.tan}(\theta) = 1 \quad \text{so} \quad \text{h}\frac{d\theta}{\cos^2\theta} = dl$$

$$\text{and } \rho = \frac{h}{\cos\theta}$$

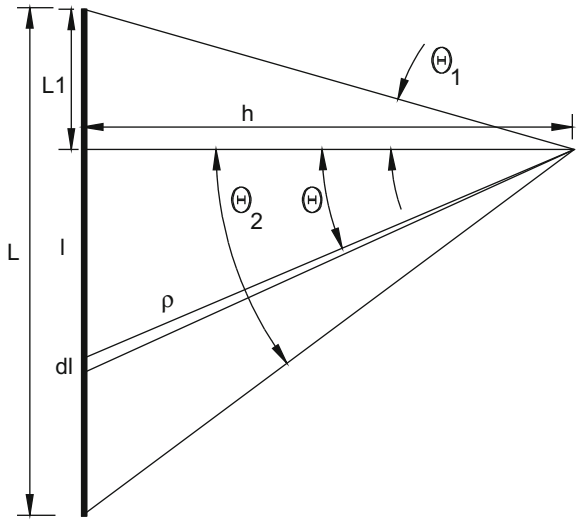

Fig. 1.22 Geometry for the calculation of the fluence of a line

we can deduce

$$d\dot{\Phi} = \frac{n_L\left(\frac{h}{\cos^2\theta}\right)}{4\pi\left(\frac{h}{\cos\theta}\right)^2} d\theta$$

to consider all of geometry, then it should be integrated across the line. hence:

$$\dot{\Phi} = \int_L d\dot{\Phi} = \frac{\dot{N}}{4\pi Lh} \int_{-\theta_1}^{\theta_2} d\theta = \frac{\dot{N}}{4\pi Lh}\left(Arc\tan\left(\frac{L_1}{h}\right) + Arc\tan\left(\frac{L-L_1}{h}\right)\right) \quad (1.59)$$

Note that when L is very small in front h, angles θ_1 and θ_2 are small and we have in this case $\arctan(\theta) \approx \theta$ when θ is small. The (1.59) becomes:

$$\dot{\Phi} = \frac{\dot{N}}{4\pi Lh}\left(Arc\tan\left(\frac{L_1}{h}\right) + Arc\tan\left(\frac{L-L_1}{h}\right)\right) \cong \frac{\dot{N}}{4\pi Lh}\left(\frac{L_1}{h} + \frac{L-L_1}{h}\right) = \frac{\dot{N}}{4\pi h^2}$$

then we find the fluence rate of a point source.

Further Details 1.2 presents an approach leading to the calculation of the fluence for a surface source.

In Chap. 2 below, we will aim at determining, for different types of conventional radiation, correlation factors "fluence-dosimetric quantity" defined by the expressions (1.48). Thereafter, metrology elements for measuring devices with suitable three quantities that are Φ, K and D will be provided.

Further Details 1.1: Distribution frequency and dose for the calculation of microdosimetric spectra

The specific energy z may be deposited via a single or multiple events. A unitary distribution is a distribution that only record the energy deposition of a single event, i.e. when a single particle and its secondary particle set in movement deposit their energy in the sensitive site. The "unitary frequency distribution" is denoted $f_1(z)$. Note that unlike $f_1(z = 0, \bar{D})$ the singularity $f_1(z = 0)$ is not defined, since by definition, for each event corresponds a deposit of energy. This distribution as the previous (1.7) is normalized to 1. The cumulative probability density $F_1(z)$ reflects the probability that the specific energy z is less than z.

$$F_1(z) = P(0 < z' \leq z, n = 1) \Rightarrow f_1(z) = \frac{dF_1(z)}{dz} \quad (1)$$

Note that this distribution of simple events is independent of the dose (i.e. the mean number of ionizations and excitations in matter), but it depends on the "typology" of energy deposition induced by radiation, the shape, size and composition of the target volume. The distribution $f_1(z)$ while discrete, can be viewed as a histogram of frequency of specific energies during the passage of a particle in the

sensitive volume. We can thus obtain a mean value called "mean specific energy frequency" as expressed by (2).

$$\bar{z}_f = \int_0^\infty z f_1(z) dz \tag{2}$$

As the value of $\bar{z}_f$ is the mean specific dose deposited by event. For a total deposited dose $\bar{D}$, the number of events can be estimated by the expression (3).

$$\bar{n} = \frac{\bar{D}}{\bar{z}_f} \tag{3}$$

These distributions are calculated by a uniform sampling of many spheres (sensitive sites) centered on the deposit points in the middle. This amounts to a uniform sampling of irradiated environment and results in "frequency distribution". This method is costly in computation time, especially for high doses.

Using a weighted sampling method, the deposited energy, as expressed in the integration, reduces the computation time and then we get the "dose distributions." In this case, the random sampling of the spheres is done with probability proportional to the energy deposited in these spheres.

The integrand of the expression (2) $zf_1(z)\mathrm{d}z$ reflects the contribution to the total deposited dose $\bar{D}$ of events depositing a specific energy between z and $z + \mathrm{d}z$. The dose distribution is then expressed in terms of the unitary frequency distribution of the expression (2) above.

$$\frac{z f_1(z)}{\bar{z}_f} dz \tag{4}$$

It reflects the fraction of the total deposited dose $\bar{D}$ which contribute to the deposits of specific energy between z and $z + \mathrm{d}z$. In other words, it is an infinitesimal increment of the total deposited dose. This relationship allows to introduce a new distribution of the specific energy, "unitary dose distribution" $d_1(z)$ defined by the expression (5).

$$d_1(z) = \frac{z f_1(z)}{\bar{z}_f} \tag{5}$$

From this distribution, which is normalized, we can calculate a second average called "mean specific energy in dose" $\bar{z}_D$.

$$\bar{z}_D = \int z\, d_1(z) dz = \int \frac{z^2 f_1(z)}{\bar{z}_f} dz = \frac{\overline{z_f^2}}{\bar{z}_f} \tag{6}$$

The index D indicates that it is an mean dose. The two calculated average $\bar{z}_f$ and $\bar{z}_D$ express two different views: $\bar{z}_f$ is the average of the specific energy deposited by each event, but events that contribute most to the dose deposit around a specific energy $\bar{z}_D$. These distributions can be calculated by simulating tracks by Monte Carlo particle transport code.

To illustrate the differences between all these microdosimetric variables, Dabli [13] offers the following schematic numerical application.

The disks in Fig. 1 represent the six spheres (sensitive sites) of an irradiated medium, randomly sampled, and the lines represent the paths of the particles (event).

If we consider that the specific energy distributed in the figure have the following values:

$$z_1 = 0.1 \text{ Gy}, \quad z_2 = 0.3 \text{ Gy}, \quad z_3 = 0.5 \text{ Gy}$$

The probability distribution of $f(z, \bar{D})$ expression (1.7) is discrete and can be summerize as follows:

$$f(0, \bar{D}) = 2/6, \quad f(z_1, \bar{D}) = 2/6, \quad f(z_2, \bar{D}) = 0/6, \quad f(z_3, \bar{D}) = 1/6,$$
$$f(z_1 + z_2, \bar{D}) = 1/6$$

Then the total deposited dose $\bar{D}$ is obtained by the expression (1.8):

$$\bar{D} = \bar{z} = \sum_i z_i f(z_i, \bar{D}) = [(3z_1 + z_2 + z_3)/6] = 0.183 \text{ Gy}$$

For the calculation of the unitary frequency distribution $f_1(z)$, only the spheres containing an energy deposition are recognized and the deposited specific energy stems from a single event. Therefore the components $f_1(0)$ and $f_1(z_1 + z_2)$ do not exist. This distribution thus can be summerize as follows:

$$f_1(z_1) = 3/5, \quad f_1(z_2) = 1/5, \quad f_1(z_3) = 1/5$$

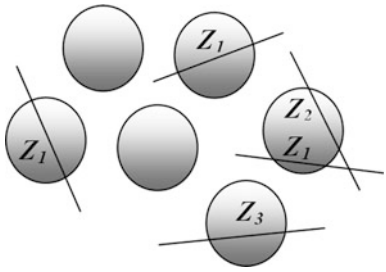

Fig. 1 Illustration for calculating distributions of specific energy [13]

the number of total events is 5. The mean specific energy frequency $\bar{z}_f$ is obtained in the discrete expression:

$$\bar{z}_f = \sum_i z_i f_1(z_i) = \frac{3z_1 + z_2 + z_3}{5} = 0.22 \text{ Gy}$$

we deduce using the expression (1.16) the mean number of events:

$$\bar{n} = \frac{\bar{D}}{\bar{z}_f} = \frac{0.183}{0.22} = \frac{5}{6}$$

Note that the mean number of events is simply the ratio of the number of events by the number of spheres. The mean specific energy dose is then obtained by discrete expression:

$$\bar{z}_D = \sum_i \frac{z_i^2 f_1(z_i)}{\bar{z}_f} = \frac{z_1^2 f_1(z_1) + z_2^2 f_1(z_2) + z_3^2 f_1(z_3)}{\bar{z}_f} = 0.336 \text{ Gy}$$

We see clearly that although we have three events to 0.1 Gy, the mean specific energy dose is at 0.336 Gy, that is to say between the single events z_2 = 0.3 and z_3 = 0.5 Gy. These events that contribute most to the dose.

Note that the methods of average calculation and distributions of specific energy z detailed above also apply to energy lineal since the latter is also subject to statistical fluctuation. However, it is notable that, by definition, the probability density function is a unitary distribution, because the values of y result only from a single event. By analogy, then, the following relations are obtained:

$$\text{Frequency unitary distribution}: f_1(y) = \frac{dF_1(y)}{dy} \tag{7}$$

$$\text{Mean lineal energy Frequency}: \bar{y}_f = \int_0^\infty y f_1(y) dy \tag{8}$$

$$\text{Dose distribution}: d(y) = \frac{y f_1(y)}{\bar{y}_f} \tag{9}$$

$$\text{Mean lineal energy dose}: \bar{y}_D = \int_0^\infty y d_1(y) dy = \int_0^\infty \frac{y^2 f_1(y)}{\bar{y}_f} dy = \frac{\overline{y_f^2}}{\bar{y}_f} \tag{10}$$

As we mentioned, this microdosimetric quantity is measured by tissue equivalent proportional counter (CPET) for example. As in the case of the specific energy, the dose distribution for lineal energy reflects the increment of the total deposited dose $\bar{D}$. Moreover, for each energy value lineal y will match a deposited dose value $D(y)$ in the medium. Knowing therefore the microdosimetric spectrum of the

distribution in dose $d(y)$, we can thus access ultimately the total dose deposited $\bar{D}$ as indicated in expression (11).

$$\bar{D} = \int_0^\infty d(y)D(y)dy = \int_0^\infty \frac{yf_1(y)}{\bar{y}_f} D(y)dy \tag{11}$$

To illustrate this approach, refer to Further Details 2.11, Chap. 2, in the section on Neutron Dosimetry.

Figure 2 shows examples of lineal energy distributions [14], represented as a frequency distribution in the left diagram or a dose distribution in the right diagram.

The lineal energy is distributed exponentially $f_1(y) = \text{Exp}\ (-y)$ with $\bar{y}_f = 1$ keV μm^{-1}. These distributions are not very different from those measured for single events in a spherical counter of 2 mm diameter simulating tissue and irradiated with ^{60}Co. In the lower part of the figure, the ordinates were multiplied by y so that the area under the curve is proportional to the fraction of events (or dose) in the considered air. Finally, we will note that, as with the digital application, the value of the mean frequency $\bar{y}_f$ is less than the mean dose $\bar{y}_D$.

Further Details 1.2: Calculating the fluence of a disk

Calculate the fluence of a disc emitting homogeneously N particle per second, of radius R at a distance D. Figure 1 shows the geometry considered.

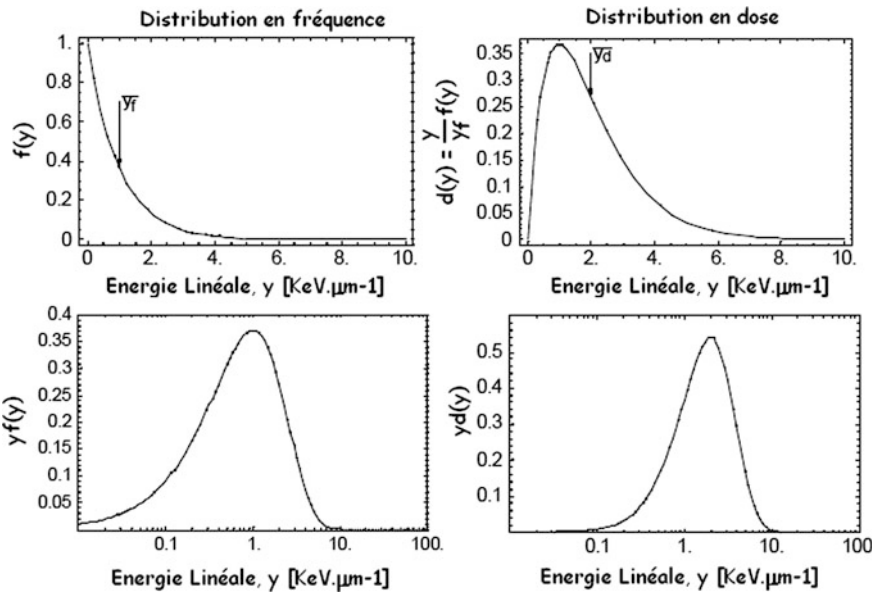

Fig. 2 Illustration of distributions and dose frequency, according [14]

At first, the disc is divided into infinitesimal elements of surface dS, so that each element dS is punctual toward the measurement point. Surface dS flux density is given as follows:

$$n_s = \frac{\dot{N}}{S} = \frac{\dot{N}}{\pi R^2}$$

The differential element fluence is expressed, toward this surface let flux density, according to:

$$d\dot{\Phi} = \frac{n_s}{4\pi\rho^2} dS$$

For a total fluence due to disk, you must integrate this equation over the full surface S:

$$\dot{\Phi} = \iint_S \frac{n_s}{4\pi\rho^2} dS \tag{1}$$

Looking at Fig. 1, the following three equations are obtained:

$$dS = r\, dr\, d\alpha, \tag{2}$$

$$\rho = \frac{D}{\cos\theta} \tag{3}$$

and

$$D\tan(\theta) = r \tag{4}$$

Differentiating on both side (4) leads to:

$$\frac{D}{\cos^2(\theta)} d\theta = dr \tag{5}$$

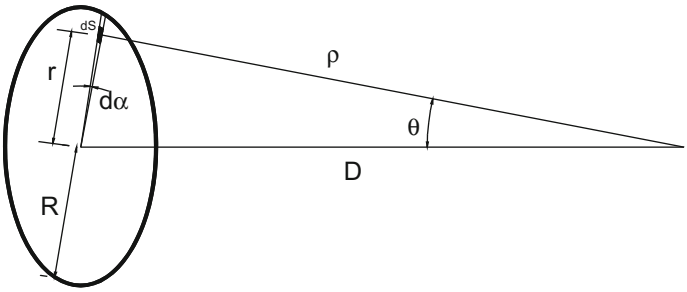

Fig. 1 Geometric consideration for exercise: calculate the fluence of a disk

Injecting (2), (4) and (5) into (1) we have:

$$\dot{\Phi} = \frac{n}{4\pi}\iint_S r\left(\frac{D}{\cos\theta}\right)^{-2} d\alpha\, dr = \frac{n}{4\pi}\iint_S \left[D\tan(\theta)\times\frac{D}{\cos^2(\theta)}\right]\left(\frac{D}{\cos\theta}\right)^{-2} d\alpha\, d\theta$$

$$= \frac{n}{4\pi}\int_0^{2\pi} d\alpha \int_0^{\arctan\left(\frac{R}{D}\right)} \tan(\theta)d\theta = \frac{n}{2}\left[-\ln\left|\cos(\theta)\right|\right]_0^{\arctan\left(\frac{R}{D}\right)}$$

finally:

$$\dot{\Phi} = \frac{N}{2\pi R^2}\left(-\ln\left|\cos\left(\arctan\left(\frac{R}{D}\right)\right)\right|\right)$$

Note that $\arctan(\theta) = \arccos\left(\left(\sqrt{(1+\theta^2}\right)^{-1}\right)$, we obtain:

$$\dot{\Phi} = \frac{\dot{N}}{2\pi R^2}\left[-\ln\left(\left(\sqrt{1+\left(\frac{R}{D}\right)^2}\right)^{-1}\right)\right] = \frac{\dot{N}}{4\pi R^2}\ln\left|\left(1+\left(\frac{R}{D}\right)^2\right)\right|$$

It is relevant to determine how for the disk can be likened to a point: remember that $\lim_{x\to 0}(\mathrm{Ln}(1+x)) = x$ (for $x = 0.1$, this approximation results in a relative error of less than 5%), which reduces the previous expression as follows:

$$\lim_{R/D\to 0}\dot{\Phi} = \frac{\dot{\mathrm{N}}}{4\pi\,\mathrm{R}^2}\left(\frac{R}{D}\right)^2 = \frac{\dot{\mathrm{N}}}{4\pi\,\mathrm{D}^2}$$

We observe the same fluence rate of a point source at a distance D. So, for a disc comparable to a point, it is necessary that $R/D \leq 0.1$ and therefore $D \geq 10\ R$.

References

1. Pouget, J. P., & Mather, S. J. (2001). General aspect of the cellular response to low and high-LET radiation. *European Journal of Nuclear Medicine, 28*, 541–561.
2. Rossi, H. H. (1979). The role of microdosimetry in radiobiology. *Radiation and Environmental Biophysics, 17*, 29–40.
3. ICRU. (1983). Microdosimetry, international commission on radiation units and measurements. Report 36.
4. ICRP. (1991). 1990 Recommendations of the international commission on radiological protection. ICRP Publication 60.

5. Bordy, J. (1992). Contribution à la réalisation d'un compteur proportionnel à dérive équivalent-tissu destiné à la dosimétrie individuelle et la radioprotection. Rapport CEA-R-5603.
6. Hanu, A., Byun, S. H., & Prestwich, W. V. (2010). A Monte Carlo simulation of the microdosimetric response for thick gas electron multiplier. *Nuclear Instruments and Methods A, 622*(1), 270–275.
7. De Choudens, H., Troesch, G. (1997). *Radioprotection dans les installations nucléaires*. Technique & Documentation.
8. Tubiana, M., Dutreix, J., Wambersie, A. (1986). *Radiobiologie*. Hermann.
9. Barendsen, G. W. (1968). Responses of cultured cells, tumours and normal tissues to radiations of different linear energy transfer. In M. Ebert & A. Howard (Eds.), *Current Topics in Radiation Research Quarterly* (Vol. IV, pp. 293–356). New York: John Wiley and Sons, Inc.
10. Wambersie, A., Menzel, H. G., Gahbaur, R. A., et al. (2002). Biological weighting of absorbed dose in radiation therapy. *Radiation Protection Desimetry, 99*, 445–452.
11. ISO. (2002). Norme internationale 8529-1. Rayonnements neutroniques de référence. Partie 1: Caractéristiques et méthode de production.
12. Delacroix, D., Guerre, J. P., Leblanc, P. (2006). *Guide pratique. Radionucléides et radioprotection. Manuel pour la manipulation de substances radioactives dans les laboratoires de faible et moyenne activité.* EDP Sciences.
13. Dabli, D. (2010). Utilisation d'un modèle microdosimétrique cinétique (MKM) pour l'interprétation d'irradiations cellulaires dans le cadre de l'hadronthérapie: Application de simulations Monte-Carlo. *Thèse Université de Clermont-Ferrand II*.
14. Francis, Z. (2007). Simulations Monte-Carlo et étude microdosimétrique pour des irradiations cellulaires à faibles doses en neutrons de 14 MeV. *Thèse Université de Clermont-Ferrand II*.
15. Faussot, A. (2009). Grandeurs et unités dosimétriques. *ATSR, 4*.
16. ICRU. (2000). Nuclear data for neutron and proton radiotherapy and for radiation protection. Report 63.

http://www.springer.com/978-3-319-48658-1

Applied Physics of External Radiation Exposure
Dosimetry and Radiation Protection
Antoni, R.; Bourgois, L.
2017, XV, 470 p. 277 illus., 21 illus. in color., Hardcover
ISBN: 978-3-319-48658-1